



Superhydrophobic melamine sponge prepared by radiation-induced grafting technology for efficient oil–water separation

Ying Sun^{1,2} · Wen-Rui Wang^{1,2} · Dan-Yi Li^{1,2} · Si-Yi Xu^{1,2} · Lin Lin^{1,2} · Man-Li Lu^{1,2} · Kai Fan³ · Chen-Yang Xing⁴ · Lin-Fan Li^{1,2} · Ji-Hao Li^{1,2}

Received: 13 November 2023 / Revised: 27 December 2023 / Accepted: 2 January 2024 / Published online: 28 August 2024

© The Author(s), under exclusive licence to China Science Publishing & Media Ltd. (Science Press), Shanghai Institute of Applied Physics, the Chinese Academy of Sciences, Chinese Nuclear Society 2024

Abstract

This paper presents a superhydrophobic melamine (ME) sponge (ME-g-PLMA) prepared via high-energy radiation-induced in situ covalent grafting of long-alkyl-chain dodecyl methacrylate (LMA) onto an ME sponge for efficient oil–water separation. The obtained ME-g-PLMA sponge had an excellent pore structure with superhydrophobic (water contact angle of 154°) and superoleophilic properties. It can absorb various types of oils up to 66–168 times its mass. The ME-g-PLMA sponge can continuously separate oil slicks in water by connecting a pump or separating oil underwater with a gravity-driven device. In addition, it maintained its highly hydrophobic properties even after long-term immersion in different corrosive solutions and repeated oil adsorption. The modified ME-g-PLMA sponge exhibited excellent separation properties and potential for oil spill cleanup.

Keywords Radiation-induced graft polymerization · Oil–water separation · Sponge · Superhydrophobic

1 Introduction

In recent years, the health of water resources and marine ecosystems has been seriously threatened by the continuous occurrence of oil spills worldwide, such as the oil spill in the Gulf of Mexico in 2010 [1] and ship collisions in the East China Sea in 2018 [2]. These accidents have had a significant impact on water resources and marine ecosystems, as

well as on the economy and human health in coastal areas, and have created many hidden dangers to normal life [3]. Therefore, solving the problem of oil–water separation is crucial for environmental protection and sustainable development. Traditional oil–water separation methods include physical (e.g., gravity separation, centrifugal separation, and filtration) and chemical (e.g., precipitation, dissolution, and adsorption) methods. However, these methods have limitations, such as low treatment efficiency, high energy consumption, high treatment costs, and secondary environmental pollution. Therefore, it is crucial to find an efficient, low-cost, and reusable material for oil–water separation [4].

To overcome the limitations of conventional methods, researchers have developed many materials such as gels [5, 6], fibers [7], foam [8], membranes [9–12], steel meshes [13] and sponges [14–16] for oil–water separation. These materials have large specific surface areas and pore structures with lipophilic or hydrophilic properties, which can accurately realize oil–water separation. Commercial sponges are widely recognized as ideal adsorbents owing to their low-cost, low density, high porosity, and excellent elastic properties [17–19]. Commercial sponges such as polyurethane typically exhibit low hydrophobicity, making it difficult to separate oil from water effectively. In contrast, the melamine

✉ Lin-Fan Li
lilinfan@sinap.ac.cn

✉ Ji-Hao Li
lijihao@sinap.ac.cn

¹ Shanghai Institute of Applied Physics, Chinese Academy of Sciences, Shanghai 201800, China

² University of Chinese Academy of Sciences, Beijing 100049, China

³ School of Architecture and Materials, Chongqing College of Electronic Engineering, Chongqing 401331, China

⁴ Center for Stretchable Electronics and NanoSensors, Key Laboratory of Optoelectronic Devices and Systems of Ministry of Education, College of Physics and Optoelectronic Engineering, Shenzhen University, Shenzhen 518060, China

and polyvinyl alcohol sponges exhibit hydrophilicity, making it easier to adsorb water molecules. These properties limit the ability of commercial sponges to separate oil and water selectively during oil–water separation. Therefore, the modification of commercial sponges to enhance their hydrophobicity is essential for the selective adsorption of oil and water.

Currently, the commonly used modification methods are generally drop coating [20], dip coating [21, 22], and chemical vapor deposition (CVD) [23] to prepare superhydrophobic sponges. Zhang et al. surface-modified a loofah sponge (LS) by chemical vapor deposition (CVD) of hydrophobic methyltrichlorosilane (MTCS). A novel oil-absorbing hydrophobic MTCS-coated loofah sponge (MTCS-LS) was successfully prepared [24]. Wu et al. prepared a TiO_2 -PVA sponge by cross-linking TiO_2 nanoparticles with H_3BO_3 and KH550, followed by chemical modification with 1H,1H, 2H, and 2H-perfluorodecyltrichlorosilane. The TiO_2 nanoparticles are firmly anchored to the surface of the pristine PVA sponge backbone [25]. Li et al. prepared a magnetic superhydrophobic melamine sponge by depositing hydrophobic magnetic nanoparticles (MNPs), synthesized by a simple drop coating method, onto a melamine sponge [17]. However, these methods typically result in noncovalent bonding between the coating and sponge surfaces. This type of coating is less stable and more susceptible to environmental and usage conditions, making it unsuitable for reuse in oil–water separation applications. In contrast, radiation grafting has many advantages for constructing superhydrophobic surfaces [26–31]. First, the synthesis conditions of the irradiation grafting method are relatively simple, requiring only the modifier to be dissolved in a suitable solvent and then irradiated with commercial sponges. This method is simple to execute, does not require complex reaction conditions, can be carried out at room temperature, and is suitable for large-scale production [32]. Irradiation grafting is a versatile technique that can be applied to various commercial sponges. This technology uses a radiation source, such as ultraviolet or gamma rays, to induce grafting reactions on surface molecules. This results in the formation of long-chain molecules with branched structures, creating a superhydrophobic surface that is highly desirable for many applications. Radiation-induced grafting is a simple method that can achieve superhydrophobicity by inhibiting contact between the liquid and solid. This method has previously been employed to graft textiles and increase their hydrophobicity. For example, Gao et al. grafted γ -methacryloyloxypropyltrimethoxysilane (MAPS) onto a cotton fabric (Co-g-PMAPS) via radiation-induced graft polymerization and successfully prepared a novel nonfluorinated organic–inorganic hybrid superhydrophobic cotton fabric [33]. Taibi et al. employed a one-step radiation-induced copolymerization method to graft linen fabrics with phosphonated and fluorinated polymer chains

using (meth) methacrylic acid monomers, resulting in modified fabrics with excellent hydrophobicity [34]. Thinko-kaew et al. grafted 2,2,2-trifluoroethyl methacrylate (TFEM) onto polypropylene (PP)-spin-bonded nonwovens using gamma irradiation to improve their hydrophobicity [35].

A commercial ME sponge was used as the substrate. We then grafted dodecyl methacrylate (LMA) with long alkyl chains onto a sponge substrate using γ -ray radiation. This process endowed the sponge with superhydrophobic properties due to the covalent bonds between the sponge and dodecyl methacrylate. These bonds also increased the hydrophobic stabilization properties of the sponge. In addition, this process had a minimal impact on the pore size of the sponge. The sponge can absorb organic solvents up to 67–168 times its weight, while maintaining a water contact angle of 149° even after ten reuses. This indicates that it has excellent recycling capabilities and significant potential in oil–water separation.

2 Experimental section

2.1 Materials

Dodecyl methacrylate (LMA), methanol, ethyl acetate, anhydrous ethanol, $\text{CuSO}_4 \cdot 5\text{H}_2\text{O}$, kerosene, dichloromethane, carbon tetrachloride, cyclohexane, and n-hexane were purchased from Sinopharm Chemical Reagent Co. Melamine sponges were purchased from Alibaba, and cooking oil and olive oil were purchased from local supermarkets.

2.2 Preparation process of ME-g-PLMA sponge

This study chose dodecyl methacrylate with long alkyl chains as the monomer for the co-irradiated grafting polymerization reaction with the ME sponge in a methanol solution.

The experimental steps were as follows: the ME sponges were washed with ethyl acetate in an ultrasonic cleaner (KQ2200E) for 20 min. Then, the sponges were dried in an electric blast drying oven (DHG-9023A) at 60° for 24 h to ensure complete dryness. The melamine sponges were then removed for subsequent processing. 0.6 mL LMA was dissolved in 20 mL of methanol solution to prepare the dodecyl methacrylate solution. Subsequently, $\text{CuSO}_4 \cdot 5\text{H}_2\text{O}$ (0.0036 g) was added to the solution and stirred until it became homogeneous. Rectangular blocks (approximately 0.09 g) measuring $2 \text{ cm} \times 2 \text{ cm} \times 3 \text{ cm}$ were cut from the cleaned ME sponges. The sponges were fully immersed in the solution, and the bottles were immediately capped after passing nitrogen gas. Finally, the bottles were sealed with a plastic tape. The ME sponge bottle underwent an irradiation reaction in the 60Co irradiation room of the Shanghai Shilong

Company. The total absorbed dose was 30 kGy, and the irradiation time was 17 h. After irradiation, the samples were removed. To eliminate the oligomers formed by the modified and unreacted monomers on the surface of the sponge, the sponge blocks were extracted in an ethyl acetate solvent for 72 h. During extraction, ethyl acetate dissolved the oligomers and unreacted monomers and washed them away from the sponge surface. Subsequently, the sponge samples are extracted and dried in an oven at 60 °C. Drying at high temperatures accelerated the volatilization of ethyl acetate and ensured complete drying of the sponge. The drying continued until the weight of the sponge sample remained constant.

2.3 Characterization

An AVATAR 370 infrared spectrometer was used to analyze the structural characteristics of the functional groups of the modified sponges. By observing the infrared absorption spectrum, we determined the chemical composition of the material and the presence of functional groups. The instrument was operated at a resolution of 4 cm⁻¹, a scanning range of 4000–600 cm⁻¹, and 32 scans. In addition, a JSM-6700F FESEM scanning electron microscope was used. SEM images were used to observe the microstructural morphologies of the virgin and modified sponges. Images were captured by accelerating the voltage to 10–15 kV, and high-resolution images were used to study the surface morphology and pore structure of the sponges. A Thermogravimetric analyzer (TGA, TG 209) was used to determine the pure ME and modified sponges' thermal stability. The heating rate was 10 °C/min under a nitrogen atmosphere up to 600 °C. The thermal decomposition characteristics of the materials were evaluated by measuring the mass changes in the samples during heating under the nitrogen atmosphere. A contact angle tester from KSV Instruments Ltd. in Finland was used. The hydrophilic and hydrophobic properties of the sponge surfaces were measured using 5 µL deionized water droplets. The wetting properties of the materials were evaluated based on the contact angles of the water droplets on the sponge surfaces. X-ray spectroscopy (ESCALAB Xi+). An X-ray electron spectrometer (ESCALAB Xi+) was used to measure changes in the elemental content of the sponges before and after modification. It was also used to determine the content and chemical status of the elements in the materials by analyzing the X-ray spectra of the samples. The experimental conditions were as follows. To measure the changes in the elemental content of the sponge before and after modification, we analyzed the X-ray spectra of the samples. This allowed the determination of the content of each element in the material and its chemical state. The experimental conditions were as follows: voltage, 8 kV; power, 30 MW; and test thickness, 3–10 nm. An electronic

universal testing machine (ETM503B) was used to measure the ability of the sponge to recover under compression. The test was conducted by applying pressure at a speed of 10 mm/min and measuring the stress–strain curve to assess the elasticity and deformability of the material.

2.4 Determination of absorption capacity

First, the mass of the ME-g-PLMA sponge was measured. The sponge was then immersed in an organic solvent and left until it fully absorbed the oil. The sponge was removed, and the organic solvent was immediately weighed to prevent reagent volatilization. The difference in the mass of the sponge before and after adsorption was recorded, and the adsorption capacity was calculated using the following formula:

$$Q = \frac{m_1 - m_0}{m_0}$$

Here, Q represents the oil absorption capacity of the sponge (g/g), and m_1 and m_0 represent the mass of the ME-g-PLMA sponge after oil absorption saturation (g) and the initial mass of the ME-g-PLMA sponge (g), respectively.

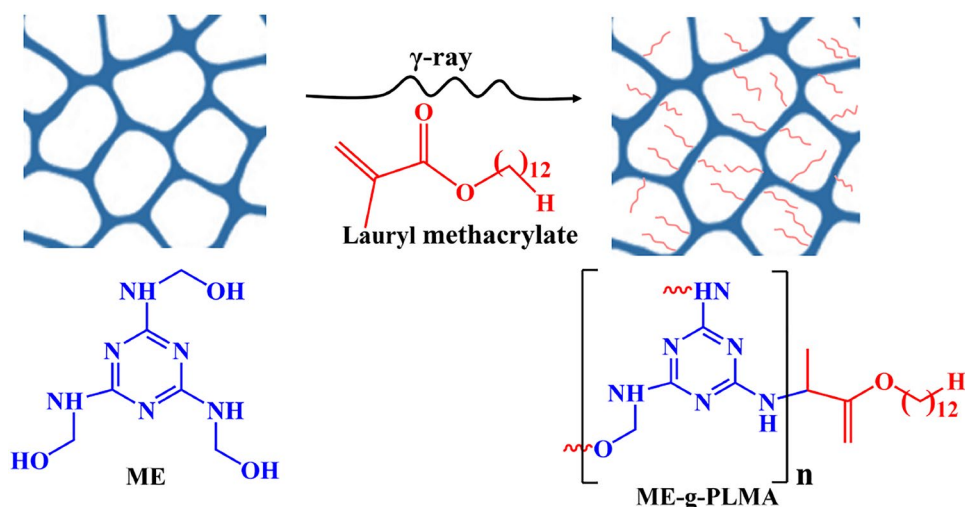
3 Results and discussion

3.1 Synthesis and characterization of the ME-g-PLMA

The graft copolymers produced by the radiation method were easier to manipulate and control than those produced by conventional chemical methods. The process is simple and efficient, enables a one-step grafting reaction, and does not require additional initiators [36]. In this study, we used co-irradiated graft polymerization to prepare ME-g-PLMA sponges. First, we chose the monomer LMA and a commercially available ME sponge with high porosity as the reactants. Then, in the methanol solution, the irradiation generated free radicals, and this polymerization reaction led to the formation of a rough layer of PLMA from LMA, which was stably loaded onto the sponge in the form of covalent bonds. Figure 1 shows a schematic of the preparation process for the ME-g-PLMA sponges.

To investigate the effect of radiation grafting modification on the morphology of ME sponges, we observed changes in their morphological characteristics before and after modification using scanning electron microscopy (SEM). As shown in Fig. 2a, b, the unmodified sponges have a three-dimensional porous structure with pore diameters ranging from 80–210 µm, a smooth surface, and low surface roughness. However, the sponges modified by radiation (Fig. 2c,d) maintained the porous structure of the original sponges and

Fig. 1 The synthetic route of ME-g-PLMA



offered a large specific surface area with a high absorption capacity. The surface of the sponge was visibly roughened, and the entire skeleton was coated with a PLMA layer. The increased roughness can effectively decrease the contact area between the water droplets and the solid surface, which plays a significant role in the selective absorption of oil and water by the sponge [22]. To confirm the occurrence of the grafting reaction, pure ME and the ME-g-PLMA sponges were analyzed using Fourier transform infrared spectroscopy (FTIR), and the results are shown in Fig. 2e. It can be observed that a new absorption peak appears near 1730 cm^{-1} in the spectrum of the modified ME sponge. This absorption peak corresponds to the telescopic vibrational absorption of the carbonyl group (C=O) in the LMA. In addition, the absorption peaks at 2854 cm^{-1} and 2925 cm^{-1} correspond to the stretching vibrations of the $-\text{CH}_2$ and $-\text{CH}_3$ groups in the modified ME sponge, respectively [37]. The appearance of these peaks indicated that the LMA monomer was successfully grafted onto the surface of the ME sponge. In order to further investigate the thermal decomposition properties of the sponges before and after modification, thermogravimetric analysis (TGA) experiments were carried out, and the thermal decomposition processes of the pure and modified ME sponges in N_2 atmosphere from 100 to $600\text{ }^\circ\text{C}$ were investigated, and the results are shown in Fig. 2f. A major mass loss of about 32.0 wt% occurred in the $372\text{--}406\text{ }^\circ\text{C}$ temperature for the pristine ME sponge. This mass loss may be due to the breakdown of the methylene bridge. In contrast, for the ME-g-PLMA sponge, a significant mass loss of about 14.2 wt% can be observed between $235\text{--}318\text{ }^\circ\text{C}$. This temperature range corresponds to the decomposition temperature of LMA homopolymers [38, 39]. In addition, the elemental content of the sponge before and after XPS characterized modification, as shown in Fig. 2g. For the original ME, it can be seen that the ME sponge has three specific peaks at 284, 397, and 531 eV, which

are attributed to the binding energies of C1 s, N1 s, and O1 s. The radiation-induced graft polymerization reaction decreases the intensity of the N1 s peak and increases the C1 s peak. Therefore, to identify the chemical composition of the sponge, the C1 (Fig. 2h) and O1s (Fig. 2i) of the sponge was also measured using XPS. The C1 s XPS spectra of the ME-g-PLMA sponges were divided into four types of carbon: $\text{C}-\text{C}_1/\text{C}_1-\text{H}$ (284.8 eV), C_2-N (285.8 eV), $\text{N}-\text{C}_3=\text{N}$ (287.3 eV), and $\text{O}-\text{C}_4=\text{O}$ (288.6 eV) [40]. By analyzing the high-resolution O1 s spectra, we observed three peaks, corresponding to $\text{O}-\text{C}=\text{O}_1$ (531.7 eV), $\text{O}_2-\text{C}=\text{O}$ (533.34 eV), and O_3-O (532.4 eV) [41, 42]. These characteristic peaks suggest that these chemical bonds may have originated from the carbonyl groups in LMA. Thus, the above synthesis demonstrates the success of graft polymerization.

3.2 Super hydrophobicity of ME-g-PLMA

Owing to its hydrophilic functional amino group, porous structure, and smooth skeleton surface, the ME sponge exhibits excellent hydrophilicity (water contact angle 0°). However, by introducing a long-alkyl-chain LMA with a low surface energy and through a radiation graft polymerization reaction, we successfully prepared the sponge material ME-g-PLMA, which exhibited excellent hydrophobicity and oil wettability. As shown in Fig. 3a, the modified sponge ME-g-PLMA exhibits hydrophobicity and floats on the water surface, whereas the pristine sponge sinks rapidly to the bottom of the beaker. When the ME-g-PLMA sponge was pressed into the water using an external force, a silver mirror-like phenomenon was observed around the ME-g-PLMA sponge (Fig. 3b). In contrast to the amphiphilic nature of the original ME sponge, the shapes of the water and oil droplets on the surface of the ME-g-PLMA sponge are shown in Fig. In Fig. 3c, we can see that the oil droplets are entirely immersed inside the sponge, whereas

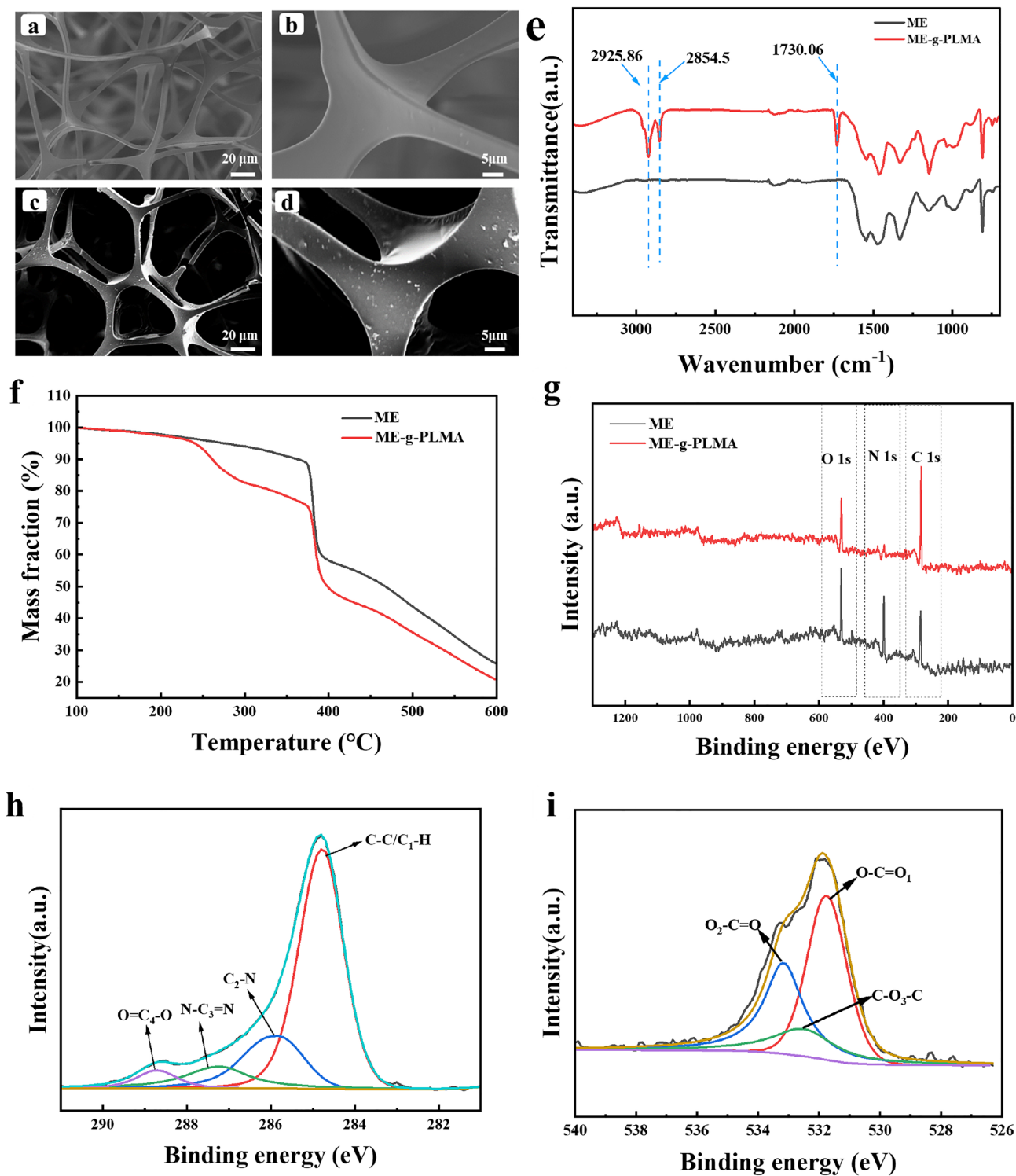


Fig. 2 SEM images of **a**, **b** ME, **c**, **d** ME-g-PLMA; **e** FTIR spectra of ME, ME-g-PLMA; **f** TGA curves of the ME and ME-g-PLMA under N_2 ; **g** XPS spectra of ME, ME-g-PLMA; **h** C 1s XPS spectra for ME-g-PLMA; **i** O 1s XPS spectra for ME-g-PLMA

all the water droplets remain spherical and roll off easily with a water contact angle of more than 150° . To further confirm graft modification inside the sponge, we tested the water contact angle inside the sponge at 155° , which was

also greater than 150° (Fig. 3d). These results indicated that by introducing a long alkyl chain LMA and performing a radial graft polymerization reaction, we successfully modified the sponge's external and internal surface properties to

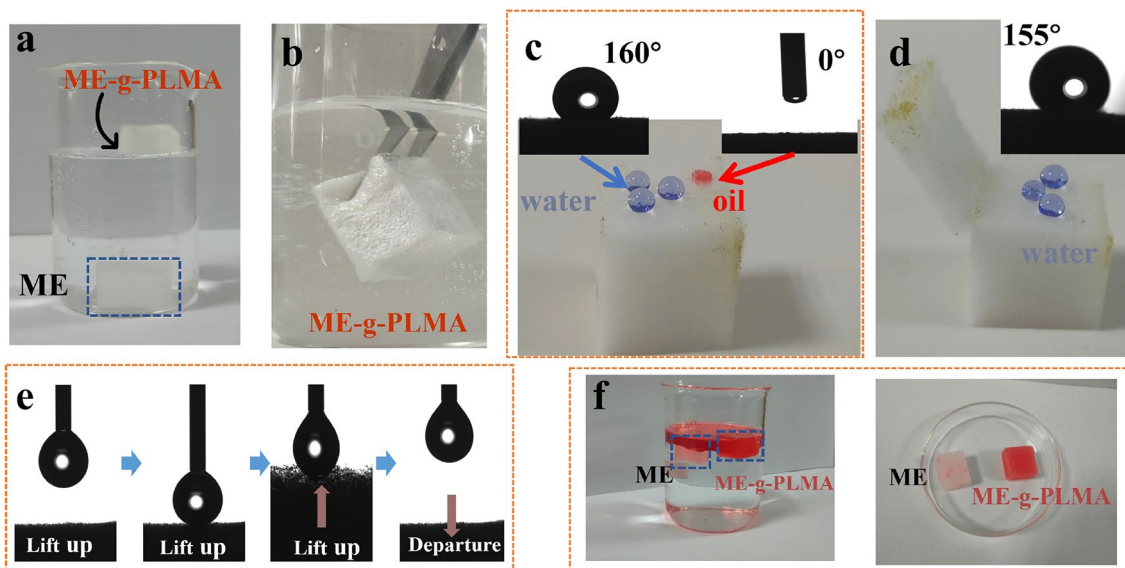


Fig. 3 **a** Photographs of the original melamine sponge and the ME-g-PLMA sponge when they were placed in the beaker; **b** Photographs of the ME-g-PLMA sponge immersed in water by external force; **c** Stained water droplets and oil droplets on the surface of the ME-g-

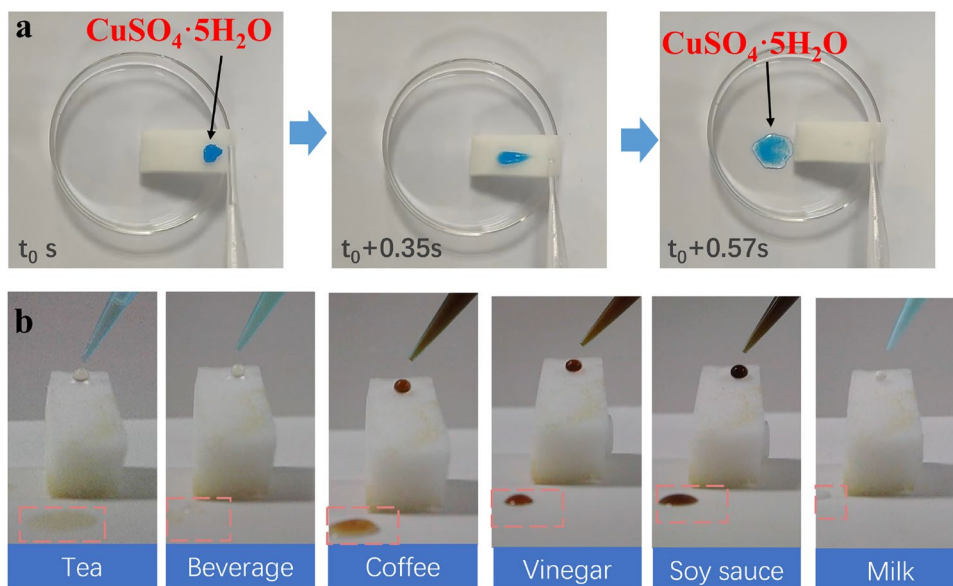
PLMA sponge; **d** Photograph of water droplets inside the ME-g-PLMA sponge; **e** Photograph of the dynamic test of water adhesion on the surface of the ME-g-PLMA sponge; **f** Photographs of the ME-g-PLMA sponge at the oil–water interface and when removed

exhibit excellent hydrophobicity and oil wettability. Interestingly, when a water droplet was forced to make contact with and move across the sponge surface, it easily slid off the superhydrophobic sponge without leaving any residual droplets (Fig. 3e). This is because of the extremely low water adhesion of the material and its porous structure. In addition, the prepared sponge exhibited no water adhesion in oil. As shown in Fig. 3f, we placed the sponge before and after modification into an oil–water mixture (cyclohexane and oil red dye were added). Although the original sponge

was lipophilic, it tended to be hydrophilic in oil and water. However, after removal, the original sponge absorbed much water, whereas the modified sponge absorbed only the top oil layer.

In addition to the large water contact angle, the spontaneous sliding property of the sponge surface is also important for oil–water separation. As shown in Fig. 4a, the hydrophilic $\text{CuSO}_4 \cdot 5\text{H}_2\text{O}$ scattered on the ME-g-PLMA sponge was continuously carried away by the water droplets and formed a clean surface within 1 s. This is due to

Fig. 4 **a** Self-cleaning ability of $\text{CuSO}_4 \cdot 5\text{H}_2\text{O}$ on the surface of the ME-g-PLMA sponge; **b** Pictures of everyday liquids rolling down on the ME-g-PLMA sponge surface



the superhydrophobicity of the sponge surface, which forms a high contact angle with the water droplets, allowing the water droplets to form a spherical shape on the sponge and quickly slide off. This spontaneous sliding property effectively removes impurities from the sponge surface and improves oil–water separation efficiency. Various solid impurities in the environment may adhere to the surface of the sponge, thus affecting the efficiency of oil–water separation. The spontaneous sliding property of the modified sponge effectively removed impurities from the sponge surface and maintained good separation performance. In addition, when other liquid droplets (e.g., tea, beverage, coffee, vinegar, soy sauce.) are dropped onto the superhydrophobic surface of the modified sponge (Fig. 4b), the droplets were repelled and rolled off the surface, which also exhibited a good separation effect. This further demonstrates the potential of the ME-g-PLMA sponge for oil–water separation applications.

3.3 Durability

Chemical stability is an important factor in characterizing the practical applications of ME-g-PLMA sponges in marine environments. To investigate the durability of ME-g-PLMA sponges, in this paper, experiments were performed using a water contact angle meter (Fig. 5a, the droplets of 1 M NaOH solution (orange-yellow staining), 3.5% NaCl solution (methyl blue staining), 0.1 M HCl (oil red staining) solution, and hot water (70 °C) are spherical on the surface of the modified sponges. The water contact angles were 150°, 146°, 147°, and 153°, all of which were greater than 145°, indicating good hydrophobicity. The change in the water contact angle of the sponge after immersion in a corrosive aqueous solution for 27 h was also investigated. The water contact angle on the sponge surface was always greater than 140° (Fig. 5b), indicating that the modified sponge has good durability and chemical stability in corrosive environments. In addition, the water contact angles of the water drops on

the sponge at different pH values indicated good hydrophobicity (Fig. 5c), and the water contact angles reached 150° and above. This verified that the radiation-modified ME-g-PLMA sponges had excellent chemical stability and maintained good hydrophobicity in harsh environments. In summary, the ME-g-PLMA sponges prepared by irradiation modification have excellent chemical stability and maintain good hydrophobic properties in harsh environments. This is of great significance for the practical application of the modified sponge in marine environments and provides a reliable basis for its application in oil–water separation, droplet separation, and other liquid treatment fields.

We conducted a detailed analysis of their surface morphologies and structural characteristics to investigate further the morphological changes in the ME-g-PLMA sponges in different corrosion solutions. Our SEM observations revealed that the sponges exhibited internal partial dissolution in both acidic and alkaline corrosion solutions but not in the NaCl solution (Fig. 6a,c and b). The surface morphology of the modified sponges was affected to varying degrees in different corrosive environments. However, the internal structure of the modified sponge remained intact, and no fractures occurred. As shown in Fig. 6d, we performed FTIR characterization of the material structure of the modified sponge. These results confirmed that the structural features of the ME-g-PLMA sponge remained unchanged. The tensile vibrational peak positions of the carbonyl groups C=O, –CH₂, and –CH₃ inside the sponge did not change significantly. This indicates that the structural features of the sponge remained stable in different corrosion solutions.

3.4 The superoleophilicity of the ME-g-PLMA

Superhydrophobic ME-g-PLMA sponges were prepared using high-energy rays to initiate graft polymerization of LMA, which was stably attached to the melamine sponges. Modifying the original ME sponges into superhydrophobic sponges without affecting their lipophilic properties is of

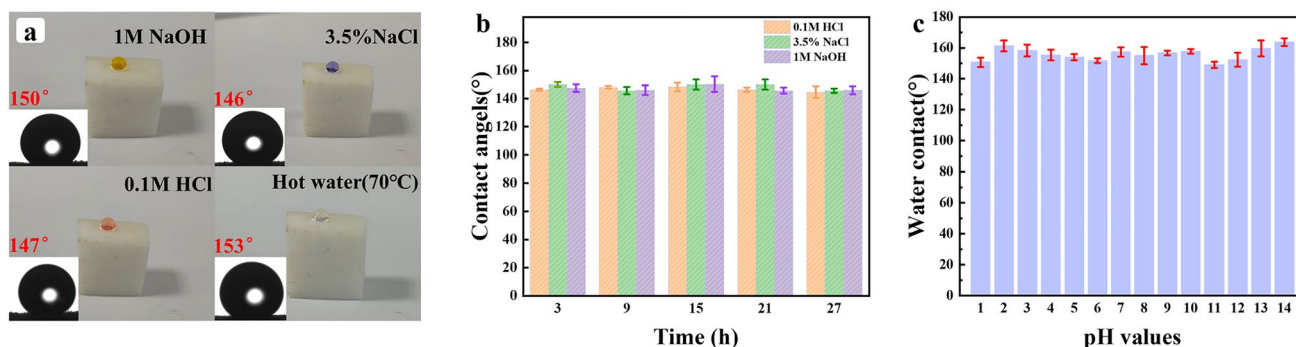
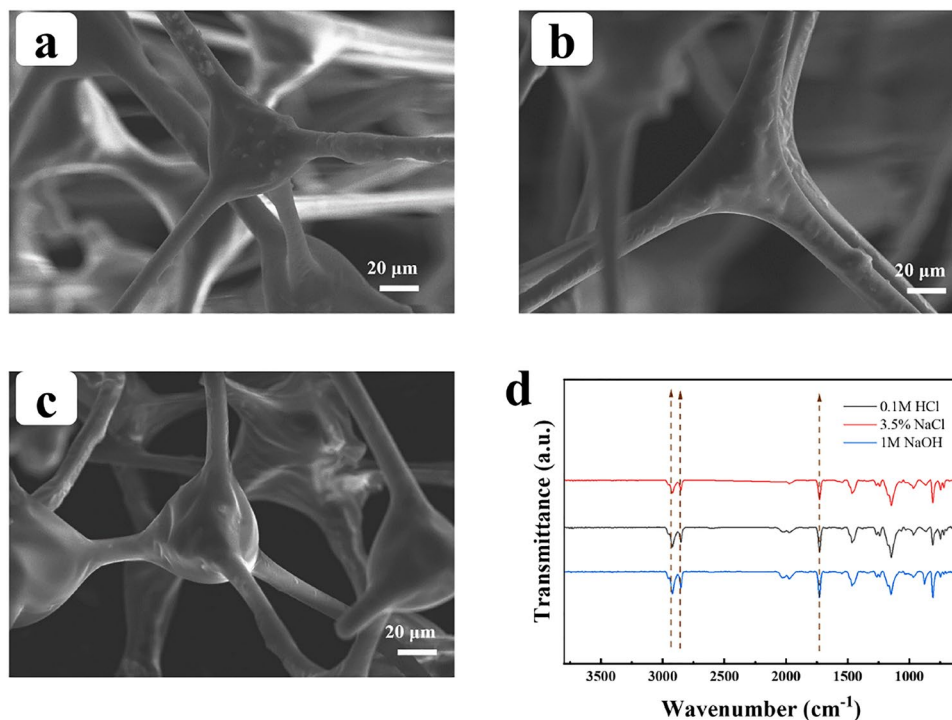


Fig. 5 **a** Pictures of droplets of 1 M NaOH, 3.5% NaCl, 0.1 M HCl, and hot water (70 °C) on the sponge surface; **b** water contact angles of ME-g-PLMA sponges after immersion in the solution for different times; **c** water contact angles of droplets of different pH values on the sponges

Fig. 6 **a** SEM image of ME-g-PLMA after immersion in 1 M NaOH solution for 27 h; **b** SEM image of ME-g-PLMA after immersion in 3.5% NaCl solution for 27 h; **c** SEM image of ME-g-PLMA after immersion in 0.1 M HCl solution for 27 h; **d** Infrared characterization of the immersed sponge



great significance in oil–water separation. The ability of the modified sponge to separate oil and water can be shown in Fig. 7a, b, which show oil red-stained carbon tetrachloride and pump oil, respectively. Owing to its higher density, the dyed carbon tetrachloride sank to the bottom of the water, whereas the sponge quickly adsorbed it when forced into the water by an external force. The dyed pump oil floats on the water surface, and the sponge quickly absorbs it when placed at the oil–water interface. Mechanical squeezing easily removed the adsorbed pump oil. The experiment demonstrated that the modified ME-g-PLMA maintained good hydrophobicity and lipophilicity both above and below the water surface and could efficiently adsorb oil from above and below the water surface. This is a valuable application

for achieving effective oil–water separation. In addition, the adsorption performance of the sponge for different organic reagents and the organic reagents, including hexane, petroleum ether, ethanol, ethyl acetate, dichloromethane, carbon tetrachloride, and oils, was investigated. As shown in Fig. 7c, the adsorption capacity of all organic reagents was more than 60 times higher, and the adsorption capacity of the sponge was positively correlated with the density of the organic reagents, with the highest adsorption capacity of carbon tetrachloride, which had the highest density of 168 g/g. Figure 7d shows that the adsorption capacity of the sponge for various oils was 81–116 times higher than that of a single sponge. The sponge also demonstrated a good adsorption capacity. Specifically, the adsorption capacity

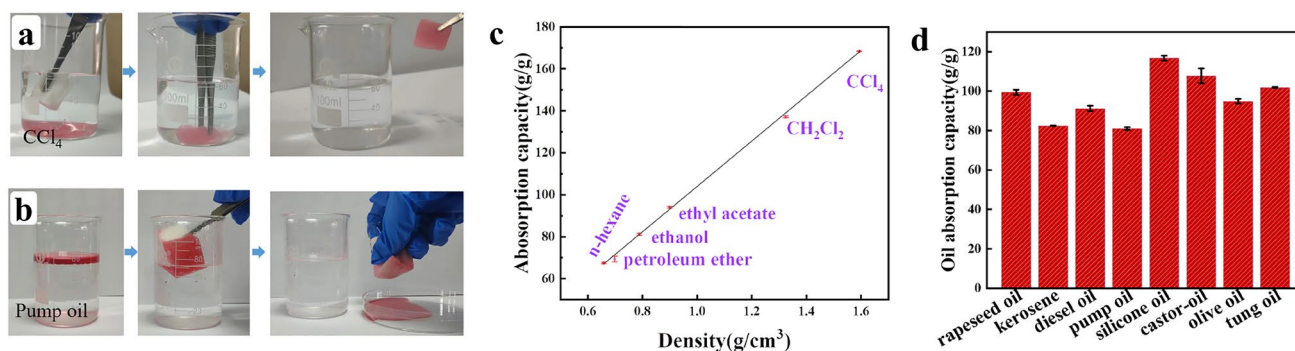


Fig. 7 **a** Picture of sponge absorbing carbon tetrachloride underwater, **b** Picture of sponge absorbing pump oil on water **c** Relationship between the ability of sponge to adsorb organic reagents and its density. **d** The ability of sponge to adsorb different oils

was 99.4 g/g for edible oil, 82.5 g/g for kerosene, 91.2 g/g for diesel, 81 g/g for pump oil, 116.8 g/g for silicone oil, 107.8 g/g for castor oil, 94.9 g/g for olive oil, and 101.9 g/g for tung oil. This was higher than those of similar melamine-modified MF/PPy sponges [43], m-CNT/PPy@MS sponges [44] and MSMS [17], and the maximum adsorption capacity for different oils ranged from 32 to 97 g/g. This excellent adsorption capacity was attributed to the sponges' highly porous structure and low density. The porous structure of the sponge offers a significant adsorption surface area, and its low density enables it to absorb considerable amounts of organic reagents and oil.

The recoverability and reusability of superhydrophobic sponges are crucial for practical applications in oil–water separation. Figure 8a shows that cyclohexane was recovered through distillation drying, and the sponge maintained its original adsorption rate even after 10 cycles, reaching 85.6 g/g. This demonstrated the sponge's excellent recovery performance. Compared with mechanical extrusion, distillation drying does not cause significant damage to the porous structure of the manufactured sponge [45]. However, this relatively inefficient recovery form may require additional time and energy. In contrast, the absorption of cyclohexane via ME-g-PLMA sponge extrusion in Fig. 8b is more convenient and environmentally friendly. This adsorption–desorption process is similar to modified

sponges such as Fe₃O₄/PDMS@MF [21] and ME/PDA/DT [43]. The adsorption capacity of the modified sponge decreased slightly after undergoing ten mechanical extrusion recycling cycles but still reached 77.1 of its original capacity. This recovery method is more efficient, allows for better control over the amount of oil recovered, and minimizes waste. Although the extrusion method did not wholly extrude all the adsorbed cyclohexane, leaving approximately 10.1 g/g of organic reagent, it was still more efficient than the distillation recovery method. In addition, Fig. 8c illustrates the minimal change in the water contact angle of the sponge after ten cycles of cyclohexane recycling. The results demonstrated that the modified sponge maintained excellent adsorption performance and reusability with a water contact angle of over 140°. The results demonstrate that the modified sponge exhibits exceptional adsorption performance and reusability, which are crucial for the long-term stabilization of the oil–water separation process and the durability of its superhydrophobic properties. It is worth noting, however, that the adsorption performance of the modified sponge decreases after several cycles of compression to absorb oil. Multiple compressions led to a loss of the mechanical properties of the sponge, which affected its adsorption capacity. The sponge model shown in Fig. 8 can withstand compression and easily return to its original state after the compression release. The grafted sponge

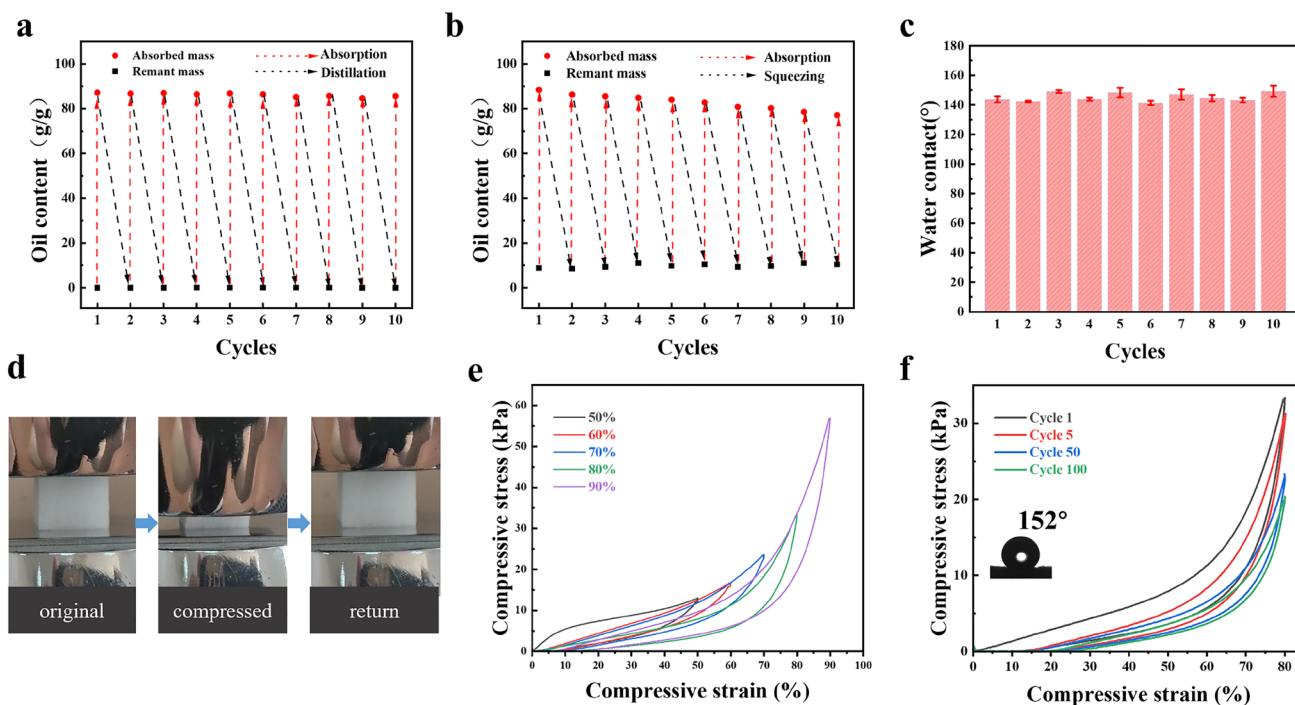


Fig. 8 Recoverable properties of ME-g-PLMA sponge absorbing cyclohexane using squeezing (a) or distillation (b); c water contact angle of the sponge under different cycles after absorbing hexane; Compression performances of the ME-g-PLMA. d Sponge compression

to reply to the image; e Compressive stress–strain (σ – ϵ) plots at various compression ϵ (50–90%); f Compressive σ – ϵ plots for up to 100 cycles at a large ϵ of 80%

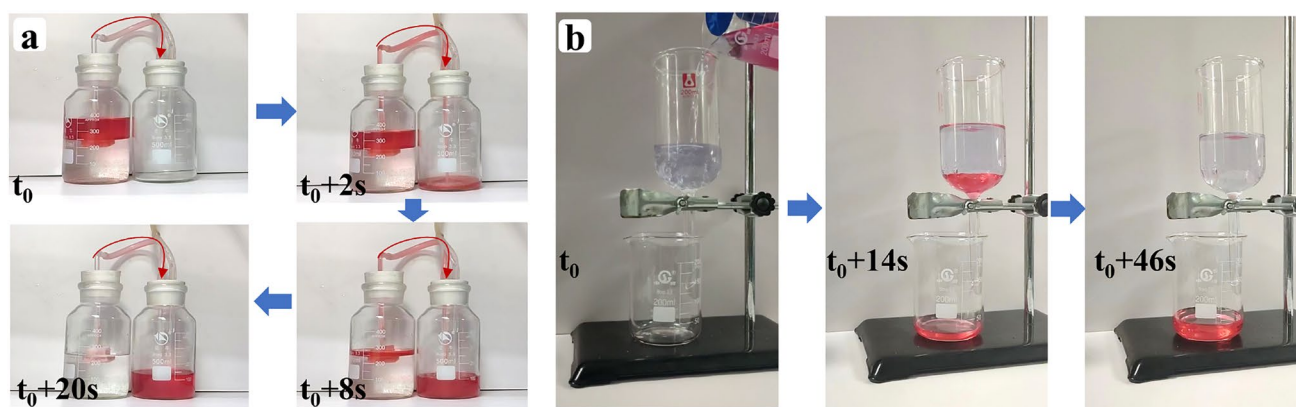


Fig. 9 **a** Device for continuous separation of hexane-water mixtures. **b** Gravity-driven separation of methylene chloride-water mixtures

underwent a significant deformation of 50–90% (Fig. 8e), demonstrating excellent recovery performance. Additionally, the superhydrophobicity of the sponge was maintained even after 100 compression cycles (Fig. 8f) and exhibited a compressible recovery ability. Compared to the PU-modified sponges, they recovered their original shapes immediately after the pressure was released, exhibiting almost no plastic deformation [46, 47]. The ME-modified sponges, on the other hand, were unable to return to their initial state fully and had a higher oil absorption capacity than other reported superhydrophobic PU sponges, with a maximum absorption capacity for various oils ranging from 10–60 g/g [20, 48, 49]. Moreover, the compression performance of the modified sponge was significantly better than that of compressible gel oil-absorbing materials, which could only be extruded to a ϵ of 50% [5]. Therefore, the modified sponge remained a reliable and long-lasting material suitable for multiple uses and recycling. In summary, the recoverability and reusability of superhydrophobic sponges are crucial for advancing oil–water separation technology.

3.5 Oil/water separation application of the ME-g-PLMA

Although hydrophobic sponges can adsorb oil at a high rate, static oil–water separation is time-consuming and inefficient and is not suitable for the separation of oily contaminants; therefore, a device that drives a pump was used to assist the sponge in achieving continuous separation of oil and water. The continuous separation process is shown in Fig. 9a, where low-density cyclohexane (stained with oil red) was poured onto the water surface, a latex tube was inserted into the modified sponge, the other end of the latex tube was inserted into the bottle, where the oil was collected, and another tube was connected to the drive pump. Once the sponge accessed the surface of the oil–water mixture, it rapidly absorbed cyclohexane, turning the pump switch on and off, and the cyclohexane was continuously absorbed

by the sponge and flowed through the tubing into the collection bottle. Eventually, the entire oil layer of the mixture was removed, leaving only the water. The average separation flow rate was 7.5 mL/s, which significantly improved the efficiency of oil–water separation and reduced the time required. The oil–water separation of light oil can be easily realized through the combination of a hydrophobic sponge and a pump. However, it is challenging to produce heavy oils underwater. We built a gravity-driven device in the second experiment (Fig. 9b). Water was stained by methyl blue, and dichloromethane was stained by oil red, and when its oil–water mixture was poured into the filtering device, due to the hydrophobicity and lipophilicity of the modified sponge, the carbon dichloride would pass through the ME-g-PLMA directly, while the blue water was blocked in the neck portion on the funnel. This phenomenon demonstrates that the modified sponge can separate oil and water mixtures by a gravity drive only, and even a small piece of the ME-g-PLMA sponge can separate a large amount of methylene chloride, which has the advantages of easy operation, low-cost, low energy consumption, and high efficiency. It is worth mentioning that the gravity-driven device was tested ten times for oil–water separation, and its excellent separation performance was still guaranteed. Compared to two-dimensional hydrophilic membrane materials [50], which can only separate light oil from water, our three-dimensional sponge structures have superior design capabilities and can continuously separate light oil from water and heavy oil from water.

4 Conclusion

In summary, a superhydrophobic and lipophilic sponge was successfully prepared by grafting LMA onto a melamine sponge in one step through a simple co-irradiation method, and its larger void structure was retained compared with the original sponge, enabling it to adsorb up to 66–168 times

its weight with high adsorption capacity, excellent reusability, self-cleaning performance, and still maintain very good hydrophobic performance, and good chemical resistance. The combination of a hydrophobic sponge and pump can easily realize the oil–water separation of light oil and improve the efficiency of oil–water separation, which can be widely used in the actual process.

Author contributions All authors contributed to the study conception and design. Material preparation, data collection and analysis were performed by Wen-Rui Wang, Dan-Yi Li and Ji-Hao Li. The first draft of the manuscript was written by Ying Sun under the guidance of Lin-Fan Li and Ji-Hao Li, and all authors commented on earlier versions of the manuscript. All authors read and approved the final manuscript.

Data availability The data that support the findings of this study are openly available in Science Data Bank at <https://cstr.cn/31253.11.sciencedb.j00186.00087> and <https://www.doi.org/10.57760/sciencedb.j00186.00087>.

Declaration

Conflict of interest The authors declare no Conflict of interest.

References

1. G.M. King, J.E. Kostka, T.C. Hazen et al., Microbial responses to the deepwater horizon oil spill: from coastal wetlands to the deep sea. *Ann. Rev. Mar. Sci.* **7**, 377–401 (2015). <https://doi.org/10.1146/annurev-marine-010814-015543>
2. Z. Yang, W. Shao, Y. Hu, Q. Ji, H. Li, W. Zhou, Revisit of a case study of spilled oil slicks caused by the sanchi accident (2018) in the East China sea. *J. Mar. Sci. Eng.* **9**, 279 (2021). <https://doi.org/10.3390/jmse9030279>
3. B. Wang, W. Liang, Z. Guo et al., Biomimetic super-lyophobic and super-lyophilic materials applied for oil/water separation: a new strategy beyond nature. *Chem. Soc. Rev.* **44**, 336–61 (2014). <https://doi.org/10.1039/C4CS00220B>
4. B. Dubansky, A. Whitehead, J.T. Miller et al., Multitissue molecular, genomic, and developmental effects of the deepwater horizon oil spill on resident Gulf Killifish (*Fundulus grandis*). *Environ. Sci. Technol.* **47**, 5074–82 (2013). <https://doi.org/10.1021/es400458p>
5. J.H. Li, J.Y. Li, H. Meng et al., Ultra-light, compressible and fire-resistant graphene aerogel as a highly efficient and recyclable absorbent for organic liquids. *J. Mater. Chem. A* **2**, 2934–2941 (2014). <https://doi.org/10.1039/c3ta14725h>
6. Y.L. He, J.H. Li, K. Luo et al., Engineering reduced graphene oxide aerogel produced by effective γ -ray radiation-induced self-assembly and its application for continuous oil–water separation. *Ind. Eng. Chem. Res.* **55**, 3775–81 (2016). <https://doi.org/10.1021/acs.iecr.6b00073>
7. S. Byun, J. Lee, J. Lee et al., Reusable carbon nanotube-embedded polystyrene/polyacrylonitrile nanofibrous sorbent for managing oil spills. *Desalination* **537**, 115865 (2022). <https://doi.org/10.1016/j.desal.2022.115865>
8. H.W. Liu, W.T. Zhai, C.B. Park, Biomimetic hydrophobic plastic foams with aligned channels for rapid oil absorption. *J. Hazard. Mater.* **437**, 129346 (2022). <https://doi.org/10.1016/j.jhazmat.2022.129346>
9. B. Xiang, J. Gong, Y. Sun et al., High permeability PEG/MXene@MOF membrane with stable interlayer spacing and efficient fouling resistance for continuous oily wastewater purification. *J. Membr. Sci.* **691**, 122247 (2024). <https://doi.org/10.1016/j.memsci.2023.122247>
10. B. Xiang, J. Gong, Y. Sun et al., Robust PVA/GO@MOF membrane with fast photothermal self-cleaning property for oily wastewater purification. *J. Hazard. Mater.* **462**, 132803 (2024). <https://doi.org/10.1016/j.jhazmat.2023.132803>
11. S.P. Gan, H. Li, X. Zhu et al., Constructing scalable membrane with tunable wettability by electrolysis-induced interface pH for oil–water separation. *Adv. Funct. Mater.* **33**, 2305975 (2023). <https://doi.org/10.1002/adfm.202305975>
12. H. Li, J.Q. Zhang, S.P. Gan et al., Bioinspired dynamic antifouling of oil–water separation membrane by bubble-mediated shape morphing. *Adv. Funct. Mater.* **33**, 2212582 (2023). <https://doi.org/10.1002/adfm.202212582>
13. H. Li, Y. Yin, L. Zhu et al., A hierarchical structured steel mesh decorated with metal organic framework/graphene oxide for high-efficient oil/water separation. *J. Hazard. Mater.* **373**, 725–732 (2019). <https://doi.org/10.1016/j.jhazmat.2019.04.009>
14. L. Liu, J. Lei, L. Li et al., A facile method to fabricate the superhydrophobic magnetic sponge for oil–water separation. *Mater. Lett.* **195**, 66–70 (2017). <https://doi.org/10.1016/j.matlet.2017.02.100>
15. Q.-R. Xiao, P. Xu, S. Sun et al., Facile fabrication of ink-based conductive hydrophobic melamine sponge for oil/water separation and oils detection. *Appl. Surf. Sci.* **604**, 154532 (2022). <https://doi.org/10.1016/j.apsusc.2022.154532>
16. Y. Wang, L. Zhou, X. Luo et al., Solar-heated graphene sponge for high-efficiency cleanup of viscous crude oil spill. *J. Clean. Prod.* **230**, 995–1002 (2019). <https://doi.org/10.1016/j.jclepro.2019.05.178>
17. Z.-T. Li, H.-T. Wu, W.-Y. Chen et al., Preparation of magnetic superhydrophobic melamine sponges for effective oil-water separation. *Sep. Purif. Technol.* **212**, 40–50 (2019). <https://doi.org/10.1016/j.seppur.2018.11.002>
18. T. Yu, F. Halouane, D. Mathias et al., Preparation of magnetic, superhydrophobic/superoleophilic polyurethane sponge: separation of oil/water mixture and demulsification. *Chem. Eng. J.* **384**, 123339 (2020). <https://doi.org/10.1016/j.cej.2019.123339>
19. P. Calcagnile, D. Fraguoli, I.S. Bayer et al., Magnetically driven floating foams for the removal of oil contaminants from water. *ACS Nano* **6**, 5413–5419 (2012). <https://doi.org/10.1021/nn3012948>
20. Z.-T. Li, B. Lin, L.-W. Jiang et al., Effective preparation of magnetic superhydrophobic Fe₃O₄/PU sponge for oil-water separation. *Appl. Surf. Sci.* **427**, 56–64 (2018). <https://doi.org/10.1016/j.apsusc.2017.08.183>
21. C. Zhang, Y. Li, S. Sun et al., Novel magnetic and flame-retardant superhydrophobic sponge for solar-assisted high-viscosity oil/water separation. *Prog. Org. Coat.* **139**, 105369 (2020). <https://doi.org/10.1016/j.porgcoat.2019.105369>
22. J. Yang, H. Wang, Z. Tao et al., 3D superhydrophobic sponge with a novel compression strategy for effective water-in-oil emulsion separation and its separation mechanism. *Chem. Eng. J.* **359**, 149–58 (2019). <https://doi.org/10.1016/j.cej.2018.11.125>
23. L. Wu, L. Li, B. Li et al., Magnetic, durable, and superhydrophobic polyurethane@Fe₃O₄@SiO₂@ fluoropolymer sponges for selective oil absorption and oil/water separation. *ACS Appl. Mater. Interfaces.* **7**, 4936–4946 (2015)
24. F. Zhang, C. Wang, J. Zhou et al., Hydrophobic sponge derived from natural loofah for efficient oil/water separation. *Sep. Purif. Technol.* **330**, 125519 (2024). <https://doi.org/10.1016/j.seppur.2023.125519>
25. Z. He, H. Wu, Z. Shi et al., Facile preparation of robust superhydrophobic/superoleophilic TiO₂-decorated polyvinyl alcohol

- sponge for efficient oil/water separation. *ACS Omega* **7**, 7084–7095 (2022). <https://doi.org/10.1021/acsomega.1c06775>
26. F. Han, W.-R. Wang, D.-Y. Li et al., Simple synthesis of silver nanocluster composites AgNCs@PE-g-PAA by irradiation method and fluorescence detection of Cr³⁺. *Nucl. Sci. Tech.* **34**, 73 (2023). <https://doi.org/10.1007/s41365-023-01224-0>
 27. F. Wang, Q.F. Wu, Y.R. Jiang et al., Effect of irradiation on temperature performance of dispersion-compensation no-core cascade optical-fiber sensor coated with polydimethylsiloxane film. *Nucl. Sci. Tech.* **33**, 11 (2022). <https://doi.org/10.1007/s41365-022-01100-3>
 28. Y.-L. He, J.-H. Li, L.-F. Li et al., The synergy reduction and self-assembly of graphene oxide via gamma-ray irradiation in an ethanediamine aqueous solution. *Nucl. Sci. Tech.* **27**, 61 (2016). <https://doi.org/10.1007/s41365-016-0068-8>
 29. X.L. Miao, J.H. Li, Q. Xiang et al., Radiation graft of acrylamide onto polyethylene separators for lithium-ion batteries. *Nucl. Sci. Tech.* **28**, 77 (2017). <https://doi.org/10.1007/s41365-017-0226-7>
 30. Y. Gu, B.W. Zhang, Z. Guo et al., Radiation-induced cross-linking: a novel avenue to permanent 3D modification of polymeric membranes. *Nucl. Sci. Tech.* **32**, 70 (2021). <https://doi.org/10.1007/s41365-021-00905-y>
 31. L. Lin, W. Wang, D. Li et al., Multifunctional graphene/Ag hydrogel with antimicrobial and catalytic properties for efficient solar-driven desalination and wastewater purification. *Chem. Eng. J.* **478**, 147249 (2023). <https://doi.org/10.1016/j.cej.2023.147249>
 32. J.X. Wu, J.Y. Li, Z.Q. Wang et al., Designing breathable superhydrophobic cotton fabrics. *RSC Adv.* **5**, 27752–27758 (2015). <https://doi.org/10.1039/c5ra01028d>
 33. Q. Gao, J. Hu, R. Li et al., Preparation and characterization of superhydrophobic organic-inorganic hybrid cotton fabrics via γ -radiation-induced graft polymerization. *Carbohydr. Polym.* **149**, 308–316 (2016). <https://doi.org/10.1016/j.carbpol.2016.04.124>
 34. M.I.M. Azzian, S.F. Mohamad, W.N.W. Salleh et al., Surface modification of PVDF membrane by radiation-induced admicellar polymerization of acrylamide in the presence of cationic surfactant. *Radiat. Phys. Chem.* **214**, 111309 (2024). <https://doi.org/10.1016/j.radphyschem.2023.111309>
 35. K. Thinkohkaew, T. Piroonpan, N. Jiraborvornpongsa et al., Radiation induced graft polymerization of fluorinated methacrylate onto polypropylene spunbond nonwoven fabric. *Surf. Interfaces* **24**, 101125 (2021). <https://doi.org/10.1016/j.surfin.2021.101125>
 36. A. Bhattacharya, B.N. Misra, Grafting: a versatile means to modify polymers: techniques, factors and applications. *Prog. Polym. Sci.* **29**, 767–814 (2004). <https://doi.org/10.1016/j.progpolymsci.2004.05.002>
 37. J. Lai, F. Guo, L. Wang et al., Poly lauryl methacrylate modified superhydrophobic Fe foam, with excellent stability and magnetic oil/water separation ability. *Mater. Chem. Phys.* **305**, 127896 (2023). <https://doi.org/10.1016/j.matchemphys.2023.127896>
 38. V.H. Pham, J.H. Dickerson, Superhydrophobic silanized melamine sponges as high efficiency oil absorbent materials. *ACS Appl. Mater. Interfaces.* **6**, 14181–14188 (2014). <https://doi.org/10.1021/am503503m>
 39. A. Iborra, L. Salvatierra, J.M. Giussi et al., Synthesis of lauryl methacrylate and poly(ethylene glycol) methyl ether methacrylate copolymers with tunable microstructure and emulsifying properties. *Eur. Polym. J.* **116**, 117–125 (2019). <https://doi.org/10.1016/j.eurpolymj.2019.04.010>
 40. G. Coullerez, D. Léonard, S. Lundmark et al., XPS and ToF-SIMS study of freeze-dried and thermally cured melamine-formaldehyde resins of different molar ratios. *Surf. Interface Anal.* **29**, 431–443 (2000). [https://doi.org/10.1002/1096-9918\(200007\)29:7<431::AID-SIA886>3.0.CO;2-1](https://doi.org/10.1002/1096-9918(200007)29:7<431::AID-SIA886>3.0.CO;2-1)
 41. G. Birlik Demirel, E. Aygül, Robust and flexible superhydrophobic/superoleophilic melamine sponges for oil–water separation. *Colloids Surf. Physicochem. Eng. Aspects* **577**, 613–621 (2019). <https://doi.org/10.1016/j.colsurfa.2019.05.081>
 42. J. Tan, Y.-F. Zhang, Trisiloxane functionalized melamine sponges for oil water separation. *Colloids Surf. Physicochem. Eng. Aspects* **634**, 127972 (2022). <https://doi.org/10.1016/j.colsurfa.2021.127972>
 43. Y. Xiang, Y. Pang, X. Jiang et al., One-step fabrication of novel superhydrophobic and superoleophilic sponge with outstanding absorbency and flame-retardancy for the selective removal of oily organic solvent from water. *Appl. Surf. Sci.* **428**, 338–347 (2018). <https://doi.org/10.1016/j.apsusc.2017.09.093>
 44. X. Wu, Y. Lei, S. Li et al., Photothermal and Joule heating-assisted thermal management sponge for efficient cleanup of highly viscous crude oil. *J. Hazard. Mater.* **403**, 124090 (2021). <https://doi.org/10.1016/j.jhazmat.2020.124090>
 45. J.T. Wang, H.F. Wang, G.H. Geng, Flame-retardant superhydrophobic coating derived from fly ash on polymeric foam for efficient oil/corrosive water and emulsion separation. *J. Colloid Interface Sci.* **525**, 11–20 (2018). <https://doi.org/10.1016/j.jcis.2018.04.069>
 46. Q. Zhu, Y. Chu, Z.K. Wang et al., Robust superhydrophobic polyurethane sponge as a highly reusable oil-absorption material. *J. Mater. Chem. A* **1**, 5386–5393 (2013). <https://doi.org/10.1039/c3ta00125c>
 47. J. Chen, M. Sun, Y. Ni et al., Superhydrophobic polyurethane sponge for efficient water-oil emulsion separation and rapid solar-assisted highly viscous crude oil adsorption and recovery. *J. Hazard. Mater.* **445**, 130541 (2023). <https://doi.org/10.1016/j.jhazmat.2022.130541>
 48. S.H. Liu, Q.F. Xu, S.S. Latthe et al., Superhydrophobic/superoleophilic magnetic polyurethane sponge for oil/water separation. *RSC Adv.* **5**, 68293–68298 (2015). <https://doi.org/10.1039/c5ra12301a>
 49. N. Cao, B. Yang, A. Barras et al., Polyurethane sponge functionalized with superhydrophobic nanodiamond particles for efficient oil/water separation. *Chem. Eng. J.* **307**, 319–325 (2017). <https://doi.org/10.1016/j.cej.2016.08.105>
 50. J. Zhang, W. Fang, F. Zhang et al., Ultrathin microporous membrane with high oil intrusion pressure for effective oil/water separation. *J. Membr. Sci.* **608**, 118201 (2020). <https://doi.org/10.1016/j.memsci.2020.118201>

Springer Nature or its licensor (e.g. a society or other partner) holds exclusive rights to this article under a publishing agreement with the author(s) or other rightsholder(s); author self-archiving of the accepted manuscript version of this article is solely governed by the terms of such publishing agreement and applicable law.